

Strong Discontinuities in the Complex Photonic Band Structure of Transmission Metallic Gratings

S. Collin, F. Pardo*, R. Teissier and J.-L. Pelouard
*Laboratoire de Microstructures et Microélectronique, CNRS UPR20,
196 av. Henri Ravera, BP 107, 92225 Bagneux CEDEX, France
(July 4, 2000)*

Complex photonic band structures (CPBS) of transmission metallic gratings with rectangular slits are shown to exhibit strong discontinuities that are not evidenced in the usual energetic band structures. These discontinuities are located on Wood's anomalies and reveal unambiguously two different types of resonances, which are identified as horizontal and vertical surface-plasmon resonances. Spectral position and width of peaks in the transmission spectrum can be directly extracted from CPBS for both kinds of resonances.

Recently, metallic films with sub-wavelength apertures became the subject of increasing interest. Experiments show that 2D arrays of sub-wavelength holes in metallic films can lead to extraordinary transmission of light [1–5]. These properties have been attributed to the excitation of coupled surface-plasmons on the upper and lower surfaces of the grating. The ability of these structures to control light has been shown [6,7], and applications have already been proposed in order to exploit these properties in different fields, such as electromagnetic filters or photolithography.

Electromagnetic calculations have been carried out by Porto *et al.* [8] in order to study the mechanisms that enhance the transmission of light through metallic gratings with very narrow slits. They distinguished two different mechanisms, that is the excitation of coupled surface plasmon polaritons on both surfaces of the metallic grating, and the coupling of incident plane waves with waveguide resonances located in the slits. They correspond respectively to surface-plasmon bands and flat bands in the energetic band structure. Similar resonances located in grooves have also been observed experimentally and numerically in the reflected light of metallic gratings [9–11].

Complex photonic band structures (CPBS) were previously calculated by Kuzmiak *et al.* for 2D periodic systems with metallic components [12], in order to obtain the attenuation and the lifetime of each mode. CPBS allowed a splitting of the lifetime of degenerate modes at Brillouin-zone boundaries to be observed.

In this Letter, we will show that, in the case of rectangular metallic gratings, complex dispersion curves demonstrate the existence of a new kind of discontinuities. Much stronger than for 2D periodic systems, they are located on Wood's anomalies. They correspond to the transition between two different types of resonances, identified as horizontal and vertical surface-plasmon resonances. The first one is a periodic structure resonance, the second one is a Fabry-Perot like resonance. The discontinuity can be up to four orders of magnitude. Moreover, we will see on zero-order transmission spectra that the calculated complex frequencies are in excellent accordance not only with the spectral position, but also with the width of resonances' peaks.

Fig. 1 shows the structure studied in this Letter, which is similar to the one of Porto *et al.* [8]. In the following, the period of the grating $d = 3.5 \mu\text{m}$ and the width of the slits $a = 0.5 \mu\text{m}$ will be kept constant, whereas the height h of the grating will vary. It is a symmetric structure, surrounded with air. The metal is assumed to be gold, whose dielectric function is taken from the reference used by Porto [13].

Our calculations were carried out for the TM polarization (the incident magnetic field is parallel to the direction y of the grating, see Fig. 1). They are based on the exact modal expansion in region II [14] and S -matrices formalism. In the upper and lower regions (I and III), the electromagnetic field is expressed as superposition of plane waves $e^{i(k_x^{(n)}x \pm k_z^{(n)}z) - i\omega t}$ (Rayleigh's expansion). Their pure real wave vector component $k_x^{(n)}$, which represents the in-plane momentum of photons is given by Eq. (1):

$$k_x^{(n)} = k_x^{(0)} + \frac{2\pi n}{d}. \quad (1)$$

The two other terms $k_z^{(n)}$ and ω are complex quantities, according to the relation $(k_x^{(n)})^2 + (k_z^{(n)})^2 = (\omega/c)^2$.

For the calculation of CPBS, we use a S -matrix formalism, in which the amplitude of the reflected and transmitted diffracted waves are given by a matrix S applied to a vector containing the amplitude of the upper and lower incident waves. An electromagnetic mode is defined by the condition of the existence of a wave in the structure without any incident wave, which is equivalent to say that the inverse (S^{-1}) of the S -matrix has an eigenvalue that is null, with an eigenvector (R_n, T_n) , corresponding to an electromagnetic field in regions I and III:

$$\Psi^I = \sum_n R_n e^{[i(k_x^{(n)}x + k_z^{(n)}z) - i\omega_0 t]}, \Psi^{III} = \sum_n T_n e^{[i(k_x^{(n)}x - k_z^{(n)}z) - i\omega_0 t]}, \quad (2)$$

with $\Re(ik_z^{(n)}) \leq 0$.

For a given $k_x = k_x^{(0)}$, the electromagnetic modes are defined by complex frequencies ω_0 . The inverse of the imaginary part of the frequency provides the amplitude lifetime 2τ of the resonance [15,12], which can be associated to the dimensionless quality factor $Q = \Re(\omega_0) \tau$.

The complex dispersion curves are lines in the three-dimensional space defined by the complex frequency ω_0 of resonance modes and the parallel momentum of photons k_x . For a more comprehensive representation we are plotting two projections of ω_0 , the energy $E = \hbar \Re(\omega_0)$ and the dimensionless quality factor $Q = \Re(\omega_0)/(-2 \Im(\omega_0))$.

Fig. 2 shows the complex dispersion curves calculated for a height $h = 1.4 \mu\text{m}$. The lines on the energetic band structure (Fig. 2(a)) represents the frontier of the Wood-Rayleigh's anomalies. They correspond to the emergence (or the vanishing) of a diffracted wave in the region I or III, which wave is then at the grazing angle. These anomalies are observed on transmission spectra when the n^{th} parallel wave vector $k_x^{(n)}$ (given by Eq. (1)) is equal to the real incident wave vector k_0 .

The energetic band structure in Fig. 2(a) shows two different types of modes, whose dispersion relations have already been studied by Porto. The bands located close to Wood's anomalies, with slightly smaller energies, characterize horizontal surface-plasmon resonances. They are excited by the first non-propagating (or evanescent) diffracted wave, and their quality factors are greater than 10 and up to more than 10^4 (see Fig. 2(b)). On the other hand, flat bands represent electromagnetic modes which are almost independent of the incident angle θ , and with lower quality factors (below 20). They were previously reported as waveguide resonances [8]. We will justify further in this Letter why these resonances are more precisely vertical surface-plasmon resonances.

The most remarkable result is given by the quality factor of the upper energetic band, which is broken into three parts. Considering the point A in Fig. 2(a), we see that the energetic band is continuous whereas the quality factor's curve is discontinuous at the corresponding points A' and A'' in Fig. 2(b). On the left side of point A, the flat band corresponds to a vertical resonance with very low quality factors (of the order of 3), whereas the right side corresponds to an horizontal surface-plasmon resonance with high quality factors (up to more than 10^4). The lifetimes of the resonances are $\tau = 2.9 \text{ fs}$ at A' and $\tau = 33 \text{ ps}$ at A''.

In order to understand physically the behavior of the electromagnetic waves, it must be pointed out that the discontinuous transitions between the two types of resonance are located exactly on Wood's anomalies (point A and its symmetrical point B), so that they are linked to the emergence or the vanishing of a diffracted wave. This phenomenon can be explained in considering the energetic band structure: below Wood's anomaly, the first non-propagating (evanescent in z direction) diffracted wave ($n = +1$ at the point A and $n = -2$ at the point B) is responsible for the excitation of the horizontal surface-plasmon resonance. When the resonance crosses Wood's anomaly, the evanescent wave becomes a z -direction propagating diffracted wave (at grazing angle) which can not excite an horizontal resonance anymore, but is coupled to vertical surface-plasmons located on the vertical walls of slits. Then, we obtain a flat band which corresponds to a "weaker" resonance in the Fabry-Perot like cavity delimited by the top and bottom surfaces of the grating. This vertical resonance is coupled with the last propagating diffracted wave, thus it ends at the crossing with Wood's anomaly, where this wave vanishes.

The complex band structure in Fig. 2 has also a continuous transition between the horizontal and the vertical resonances in the lower band. The flat band at normal incidence corresponds to vertical resonances, and becomes a surface-plasmon band for greater incident angles. Its quality factor increases from 20 to about 300 during this smooth transition. The last flat band at about 0.35 eV corresponds to a vertical resonance for the whole range of k_x in Fig. 2.

By varying the width a of the slits, we have observed that the complex mode of the vertical resonance is nearly unchanged. In the calculation, it can be seen from the modal decomposition of the electromagnetic field, that this resonance corresponds mainly to the excitation of the first eigenmode of a z infinitely extended region II. The wave is evanescent in the x direction and propagates at the vertical interfaces air/metal (z direction). This TM mode exists for any width of slit, and becomes equal to the wave vector k_{ps} of the surface-plasmon of a semi-infinite air-metal interface in the limit of wide slits, so that it is more correct to call it a *vertical surface-plasmon mode* instead of a waveguide mode. The transitions between the regions II/I and II/III act as mirrors for the vertical surface-plasmon mode. Their reflection coefficients are low, so that the vertical resonance is a Fabry-Perot like resonance with low quality factors.

Complex dispersion curves shown above can be seen as convenient compact representations of the resonances, which can be associated to transmission spectra. For that purpose, we make the hypothesis that the complex frequency ω_0^i of a resonance i is a single pole of the amplitude of the transmitted waves. Consequently, the zero-order transmitted energy can be approximated by a Lorentzian function near the resonance i . Assuming ω is the (real valued) frequency of the incident wave, we obtain:

$$T_0 = \left| \frac{\alpha_i}{\omega - \omega_0^i} \right|^2. \quad (3)$$

The complex band structure of the grating is shown in Fig. 3 for a height $h = 3 \mu\text{m}$. Fig. 4 shows the zero-order transmission spectra calculated for the same height and two different angles of incidence. They correspond to $\theta = 0^\circ$ (a) and $\theta = 12^\circ$ (b) cuttings in Fig. 3(a). The Lorentzian curves corresponding to Eq. (3) are added to the spectra. The constant α_i is fitted to obtain the same maximum value as the spectra. At normal incidence (Fig. 4(a)), the broad resonances at 0.38 eV and 0.54 eV (not represented in Fig. 3) are not separated enough to allow the comparison to their respective Lorentzian functions to be made. In such a case, the amplitude of the transmitted wave is the sum of two complex Lorentzian functions, and phase considerations make it more difficult to fit to the spectra.

For the other peaks, Fig. 4 shows an excellent agreement of the Lorentzian curves with the spectra. Hence, the single-pole approximation is justified and Eq. (3) gives the width at half maximum:

$$\Delta\omega_0 = -2 \Im(\omega_0^i). \quad (4)$$

It justifies also the above definition of the quality factor of the resonance, which corresponds to the more conventional $Q = E/\Delta E$.

These transmission spectra allow some important characteristics of the resonances to be pointed out. At first, it must be noted that the flat band at about 0.35 eV has no solution at normal incidence, and the peak γ disappears at $\theta = 0^\circ$. An energetic shift can be seen for the horizontal surface-plasmon resonances between $\theta = 0^\circ$ and $\theta = 12^\circ$, whereas the vertical resonance at about 0.17 eV does not move. Another point which comes out of the calculations is that vertical resonances in contiguous slits are nearly uncoupled. As a consequence, a periodic structure is not necessary for them to exist: the vertical surface-plasmon resonance could be excited in a unique slit, and fully coupled with a few ones. Hence, an important result is that the vertical resonance can be efficiently excited by a strongly focalized beam.

In conclusion, we have carried out the calculation of the complex dispersion curves of rectangular metallic gratings in TM polarization. CPBS are directly linked to experimental data, like transmission spectra. The quality factor and the lifetime of resonances, that they provide, are crucial characteristics in many applications already proposed for the extraordinary effects appearing in such transmission metallic gratings. CPBS show pronounced discontinuities located on Wood's anomalies, which can not be evidenced in the usual energetic dispersion curves. They allow to distinguish unambiguously the two different natures of resonances: *horizontal and vertical surface-plasmon resonances*. Similar results can be obtained for reflection gratings. This work can also be extended in order to analyze resonances in more complex geometries, as Ebbesen's structures [1] for example, for which a cutoff diameter exists for vertical modes. The characteristics of the resonances studied in this Letter open up new possibilities in photonic materials. Moreover, these structures allow huge concentrations of light in very small volumes, which could have applications in fundamental optics [16] and in optoelectronics.

* email: Fabrice.Pardo@L2m.cnrs.fr

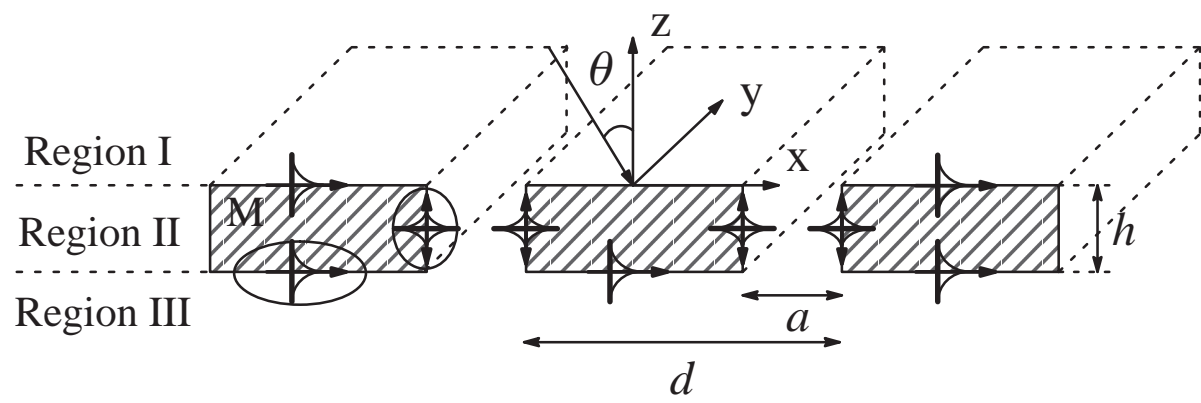
- [1] T. W. Ebbesen, H. J. Lezec, H. F. Ghaemi, T. Thio, and P. A. Wolff, *Nature* **391**, 667 (1998).
- [2] H. F. Ghaemi, T. Thio, D. E. Grupp, T. W. Ebbesen, and H. J. Lezec, *Phys. Rev. B* **58**, 6779 (1998).
- [3] T. Thio, H. F. Ghaemi, H. J. Lezec, P. A. Wolff, and T. W. Ebbesen, *J. Opt. Soc. Am. B* **16**, 1743 (1999).
- [4] D. E. Grupp, H. J. Lezec, T. Thio, and T. W. Ebbesen, *Adv. Mater.* **11**, 860 (1999).
- [5] C. Sönnichsen, A. C. Duch, G. Steininger, M. Koch, G. von Plessen, and J. Feldmann, *App. Phys. Lett.* **76**, 140 (2000).
- [6] T. J. Kim, T. Thio, T. W. Ebbesen, D. E. Grupp, and H. J. Lezec, *Opt. Lett.* **24**, 256 (1999).
- [7] T. Thio, H. J. Lezec, and T. W. Ebbesen, *Physica B* **279**, 90 (2000).
- [8] J. A. Porto, F. J. Garcia-Vidal, and J. B. Pendry, *Phys. Rev. Lett.* **83**, 2845 (1999).
- [9] T. Lopez-Rios, D. Mendoza, F. J. Garcia-Vidal, J. Sanchez-Dehesa, and B. Pannetier, *Phys. Rev. Lett.* **81**, 665 (1998).
- [10] W.-C. Tan, T. W. Preist, J. R. Sambles, and N. P. Wandstall, *Phys. Rev. B* **59**, 12661 (1999).
- [11] N. P. Wandstall, T. W. Preist, W. C. Tan, M. B. Sobnack, and J. R. Sambles, *J. Opt. Soc. Am. A* **15**, 2869 (1998).
- [12] V. Kuzmiak and A. A. Maradudin, *Phys. Rev. B* **55**, 7427 (1997).
- [13] B. Dold and R. Mecke, *Optik* **22**, 435 (1965).
- [14] P. Sheng, R. S. Stepleman, and P. N. Sanda, *Phys. Rev. B* **26**, 2907 (1982).
- [15] F. Pardo, Ph.D. thesis 86 PA11 2161, Univ. Paris-Sud Orsay (1986), <http://services.inist.fr>, 59477.
- [16] J. Pendry, *Science* **285**, 1687 (1999).

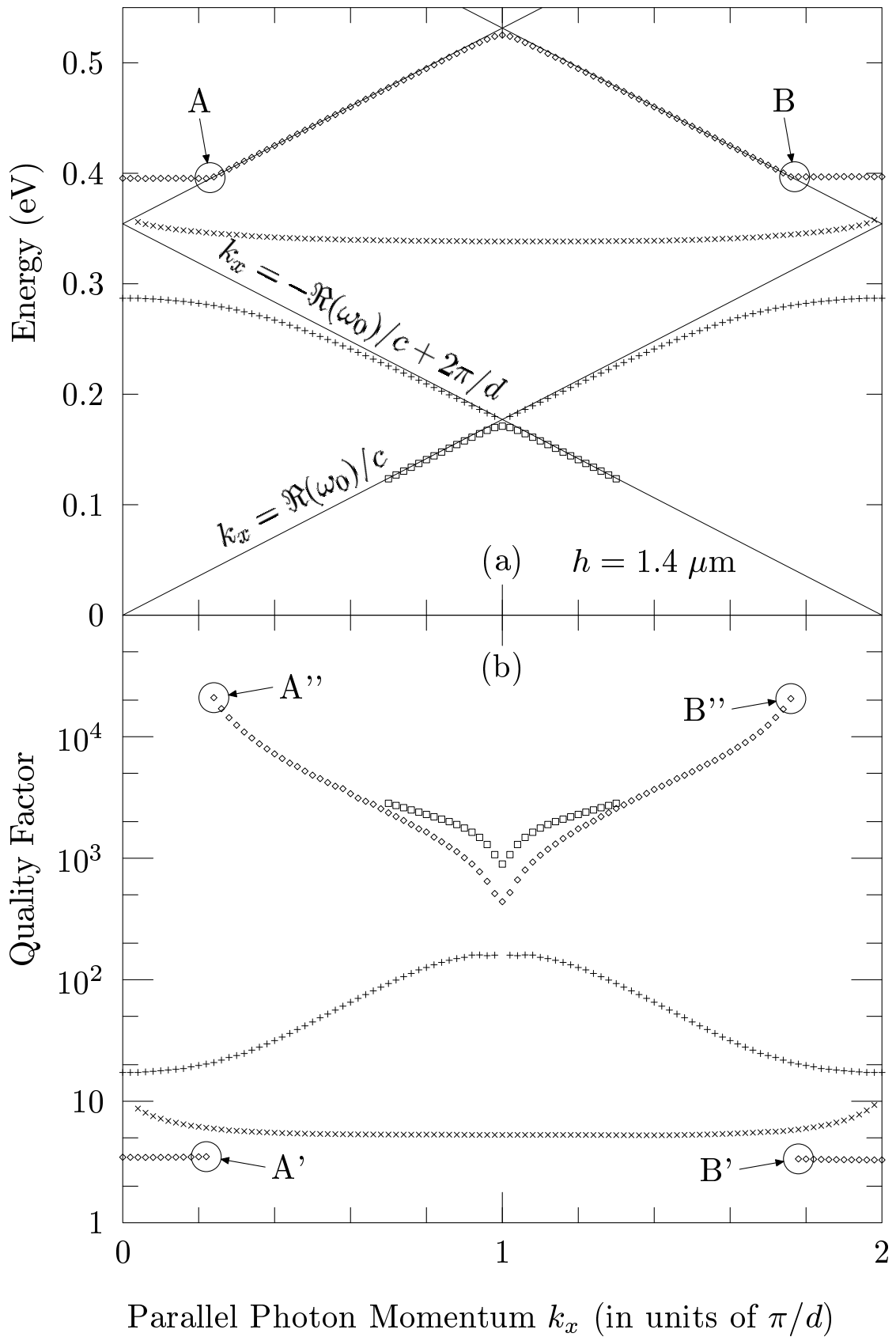
FIG. 1. Description of the metallic grating. Horizontal and vertical surface-plasmons are symbolically represented.

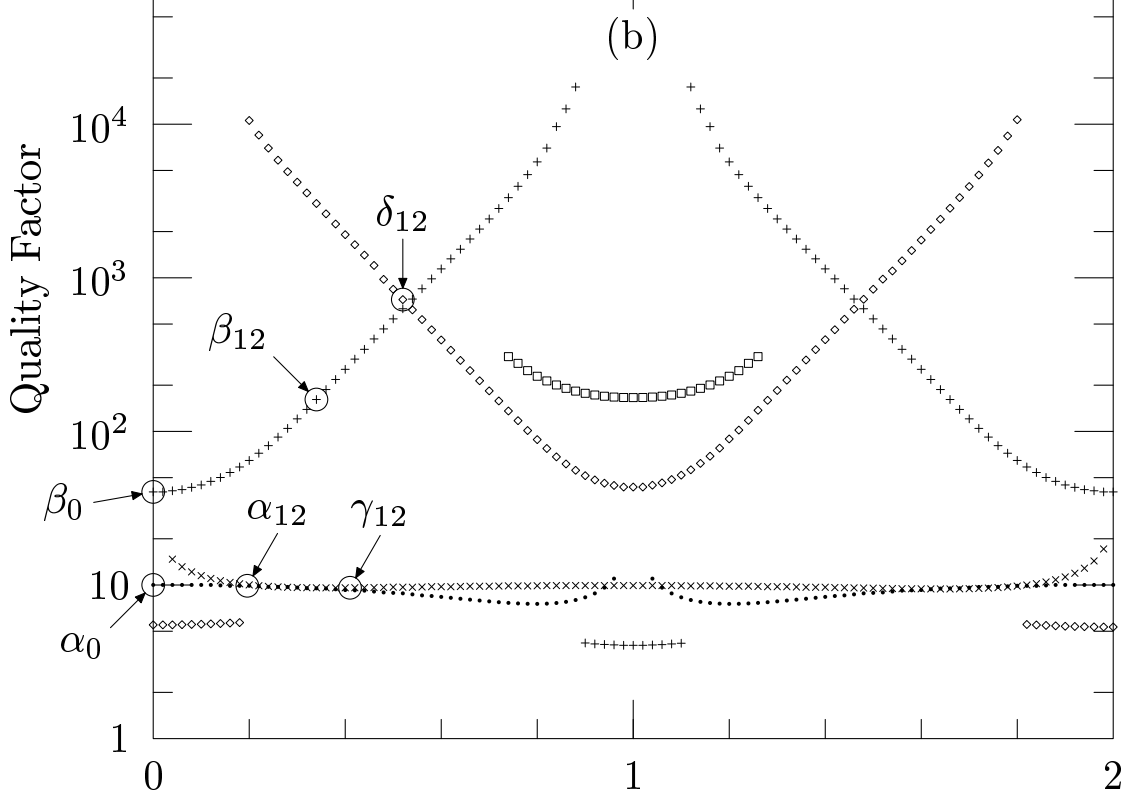
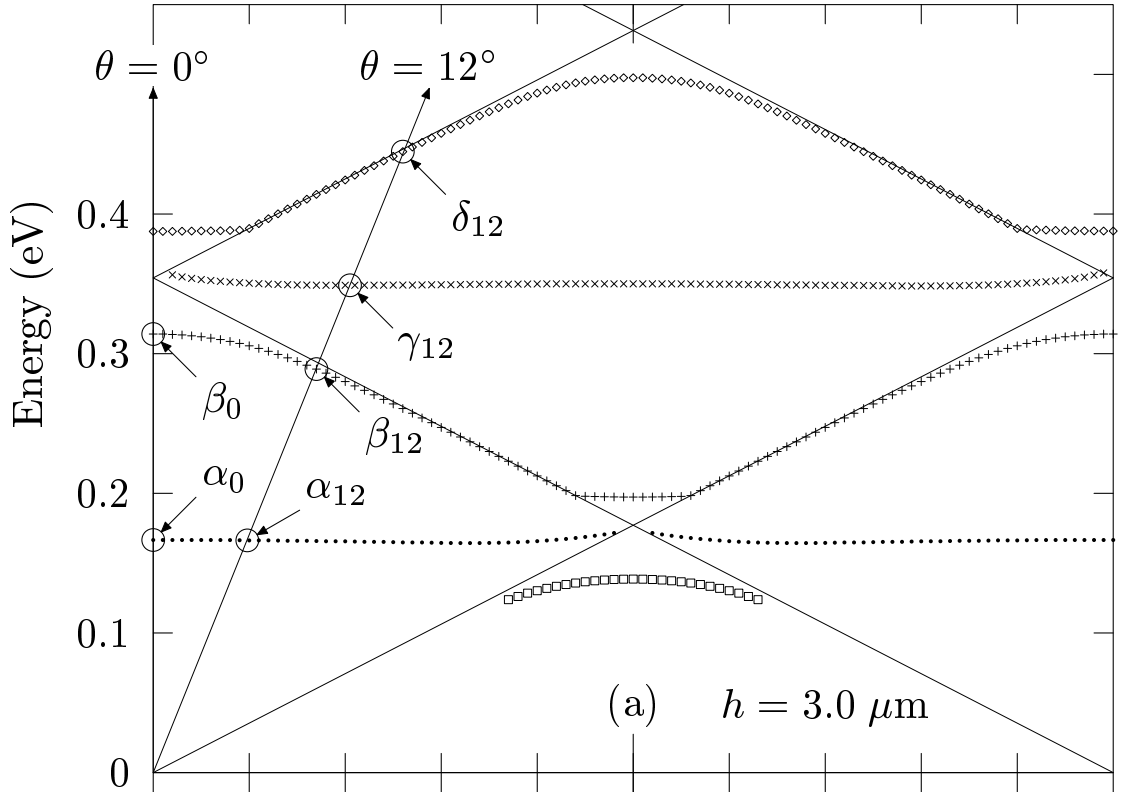
FIG. 2. Energetic (a) and quality-factor Q (b) representation of the first four photonic bands of a rectangular metallic grating ($d = 3.5 \mu\text{m}$, $a = 0.5 \mu\text{m}$) with a height $h = 1.4 \mu\text{m}$. The lower band is only computed for energies higher than 0.125 eV ($\lambda < 10 \mu\text{m}$). Wood's anomalies (lines) are added to the energetic band structure (a).

FIG. 3. Energetic (a) and quality-factor Q (b) representation of the first five photonic bands of a rectangular metallic grating ($d = 3.5 \mu\text{m}$, $a = 0.5 \mu\text{m}$) with a height $h = 3.0 \mu\text{m}$. The lower band is only computed for energies higher than 0.125 eV ($\lambda < 10 \mu\text{m}$). Wood's anomalies (lines) are added to the energetic band structure (a).

FIG. 4. Comparison between zero-order transmission spectra (solid lines) and Lorentzian curves (dotted lines) for a rectangular metallic grating ($d = 3.5 \mu\text{m}$, $a = 0.5 \mu\text{m}$, $h = 3.0 \mu\text{m}$). The angle of incidence is (a) $\theta = 0^\circ$ and (b) $\theta = 12^\circ$.







Parallel Photon Momentum k_x (in units of π/d)

